JACS
JOURNAL OF THE AMERICAN CHEMICAL SOCIETY
Communication
pubs.acs.org/JACS

Experimental Evidence of Ultrafast Quenching of the ^{3}MLCT Luminescence in Ruthenium(II) Tris-bipyridyl Complexes via a ^{3}dd State

Qinchao Sun,[†,§] Sandra Mosquera-Vazquez,[†,§] Latévi Max Lawson Daku,[†] Laure Guénée,[‡] Harold A. Goodwin,[#] Eric Vauthey,[†] and Andreas Hauser*[,†]

[†]Département de chimie physique, Université de Genève, 30 Quai Ernest-Ansermet, CH-1211 Genève 4, Switzerland
[‡]Laboratoire de cristallographie, Université de Genève, 24 Quai Ernest-Ansermet, CH-1211 Genève 4, Switzerland
[#]School of Chemical Sciences, University of New South Wales, Sydney 2052, Australia

Supporting Information

ABSTRACT: Ultrafast transient absorption spectroscopy serves to identify the ^{3}dd state as intermediate quencher state of the ^{3}MLCT luminescence in the non-luminescent ruthenium complexes $[Ru(m\text{-}bpy)_3]^{2+}$ (m-bpy = 6-methyl-2,2′-bipyridine) and $[Ru(tm\text{-}bpy)_3]^{2+}$ (tm-bpy = 4,4′,6,6′-tetramethyl-2′,2′-bipyridine). For $[Ru(m\text{-}bpy)_3]^{2+}$, the population of the ^{3}dd state from the ^{3}MLCT state occurs within 1.6 ps, while the return to the ground state takes 450 ps. For $[Ru(tm\text{-}bpy)_3]^{2+}$, the corresponding values are 0.16 and 7.5 ps, respectively. According to DFT calculations, methyl groups added in the 6 and 6′ positions of bipyridine stabilize the ^{3}dd state by ∼4000 cm^{-1} each, compared to $[Ru(bpy)_3]^{2+}$.

The effect of excited ligand-field states on the photophysical properties of ruthenium(II) polypyridyl complexes has been widely discussed.[1−5] For photovoltaic applications, the lowest energy ligand-field state has to be at higher energy than the luminescent triplet metal-to-ligand charge-transfer (^{3}MLCT) state.[6] However, a recently proposed strategy to develop drugs for anticancer therapy based on light-induced ligand dissociation via ligand-field states has led to renewed interest in the fundamental questions regarding their role.[5,7,8] In the strong ligand field of 4d^n metal ions with polypyridyl ligands, the first excited ligand-field state, the $^3T_1(t_{2g}^5e_g^1)$ state, is at an energy comparable to that of the lowest energy MLCT state. As Van Houten and Watts[9] proposed some 4 decades ago, for $[Ru(bpy)_3]^{2+}$ (bpy =2,2′-bipyridine) in H_2O, the lowest component of the ^{3}dd manifold, 3600 cm^{-1} higher in energy than the ^{3}MLCT multiplet, is held responsible for the thermally activated quenching of the ^{3}MLCT luminescence. This is still the accepted explanation not only for the parent $[Ru(bpy)_3]^{2+}$ complex but also for the large class of ruthenium(II) polypyridyl complexes,[1,2,5,10] as it explains the large variation in quenching rates observed for chemically quite similar systems. With the advent of ultrafast laser spectroscopy, the excited-state dynamics of $[Ru(bpy)_3]^{2+}$ became a prime target, and it has been established that, after initial excitation into the intense ^{1}MLCT band, intersystem crossing (ISC) takes the complex to the corresponding ^{3}MLCT state within ∼50 fs,[11,12] followed by vibrational relaxation on the 5−10 ps time scale.[13a,14] In this system, even though thermal quenching becomes important above room temperature, the signature of the ^{3}dd state is not accessible experimentally because its population as a short-lived transition state is never sufficiently high. Except for attributing short luminescence lifetimes in multidentate systems to the quenching by the short-lived ^{3}dd manifold,[15,16] to date there is no spectroscopic study of the corresponding ISC and internal conversion processes. In this Communication, we present ultrafast transient absorption spectra of $[Ru(m\text{-}bpy)_3]^{2+}$ (m-bpy = 6-methyl-2,2′-bipyridine) and $[Ru(tm\text{-}bpy)_3]^{2+}$ (tm-bpy = 4,4′,6,6′-tetramethyl-2′,2′-bipyridine) and compare them to those of $[Ru(bpy)_3]^{2+}$, thus identifying the ^{3}dd state in the two complexes as an intermediate state in the relaxation cascade.

$[Ru(bpy)_3](PF_6)_2$, $[Ru(m\text{-}bpy)_3](BF_4)_2$, and $[Ru(tm\text{-}bpy)_3](BF_4)_2$ were prepared according to standard methods (see Supporting Information (SI)). Their absorption spectra are almost identical, with the intense ^{1}MLCT band centered at ∼454 nm. The only difference is that, for $[Ru(m\text{-}bpy)_3]^{2+}$ and $[Ru(tm\text{-}bpy)_3]^{2+}$, the extinction coefficients at the band maximum are smaller. Whereas $[Ru(bpy)_3]^{2+}$ in CH_3CN solution at 295 K shows intense luminescence from the ^{3}MLCT state (λ_{max} = 610 nm, $\tau_L \approx$ 850 ns, $\eta_L \approx$ 9%),[17] the other two complexes show no luminescence at the sensitivity of the spectrometer used. Figure 1 shows the transient absorption spectra of the three compounds recorded in deoxygenated CH_3CN solutions following pulsed irradiation at 400 nm (pulse duration 80 fs, instrument response 150 fs). The series measured for $[Ru(bpy)_3]^{2+}$ shows the build-up of the transient spectrum during the pulse, with a bleaching of the ^{1}MLCT band at 454 nm (to be compared with the absorption spectrum included in Figure 1) and excited-state absorptions (ESAs) centered at 360 nm and above 500 nm. The ESA bands at 360 nm and above 500 nm have been attributed to a transition centered on bpy$^-$, that is, on the formally reduced ligand, and a ligand-to-metal charge-transfer (LMCT) transition from one of the neutral ligands to the formally oxidized Ru^{3+} ion of the ^{3}MLCT state, respectively.[13a,14,18] This spectrum decays mono-exponentially at all wavelengths with the same time constant as

Received: July 15, 2013
Published: September 3, 2013

dx.doi.org/10.1021/ja407225t | J. Am. Chem. Soc. 2013, 135, 13660−13663

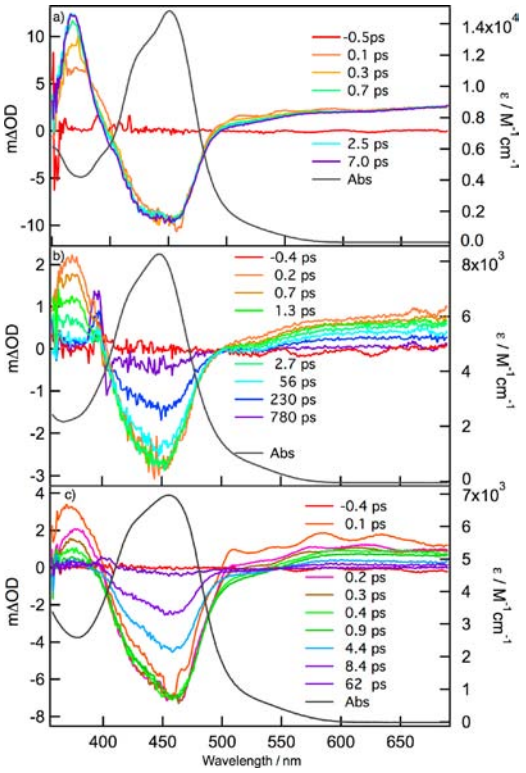

Figure 1. Transient absorption spectra at selected time delays of (a) $[Ru(bpy)_3]^{2+}$, (b) $[Ru(m\text{-}bpy)_3]^{2+}$, and (c) $[Ru(tm\text{-}bpy)_3]^{2+}$, $c = 2 \times 10^{-5}$ M, λ_{ex} = 400 nm, 3.1, 1.2, and 3.1 μJ/pulse focused on ϕ = 300 μm in CH_3CN at 295 K. For direct comparison, the corresponding absorption spectra are shown in gray (right axis).

the luminescence decay, indicating that ^{3}MLCT decay and ground-state recovery go hand in hand.

For $[Ru(m\text{-}bpy)_3]^{2+}$ and $[Ru(tm\text{-}bpy)_3]^{2+}$, the spectra at short delays are similar to that of $[Ru(bpy)_3]^{2+}$; that is, they show the characteristics typical of the ^{3}MLCT state. However, the band at 360 nm decays much faster than the ground-state recovery. The fast disappearance of the 360 nm signal indicates a depopulation of the ^{3}MLCT state. The fact that ground-state recovery is orders of magnitude slower indicates an almost quantitative population of an intermediate state.

Figure 2 shows the experimental transient profiles at 370, 454, and 630 nm for all three complexes and the results of multi-exponential global fits performed using all spectra and taking into account the instrument response function of 150 fs via iterative reconvolution. The corresponding decay-associated difference absorption spectra (DADS) are shown in Figure 3. For $[Ru(bpy)_3]^{2+}$, the fit function is $f(t) = A_1 \exp(-t/\tau_1) + A_{inf}$, because the ^{3}MLCT does not decay noticeably within the time window of t < 1 ns.[13a] The fast component with the time constant τ_1 = 1.8 ps corresponds to a combination of the ultrafast ^{1}MLCT→^{3}MLCT ISC, charge localization on one of the ligands,[13] solvent reorganization, and vibrational relaxation.[11,13a,18] The A_{inf} component corresponds to the ESA of the ^{3}MLCT state and ground-state bleaching as discussed above. For $[Ru(m\text{-}bpy)_3]^{2+}$, the fit function is $f(t) = A_1\exp(-t/\tau_1) + A_2\exp(-t/\tau_2)$. The DADS show that the 360 nm ESA characteristic for the ^{3}MLCT state decays with τ_1 = 1.6 ps, whereas the ground-state recovery occurs with τ_2 = 450 ps. For $[Ru(tm\text{-}bpy)_3]^{2+}$, a global fit to the transient absorption spectra was not possible, as, in addition to the electronic processes,

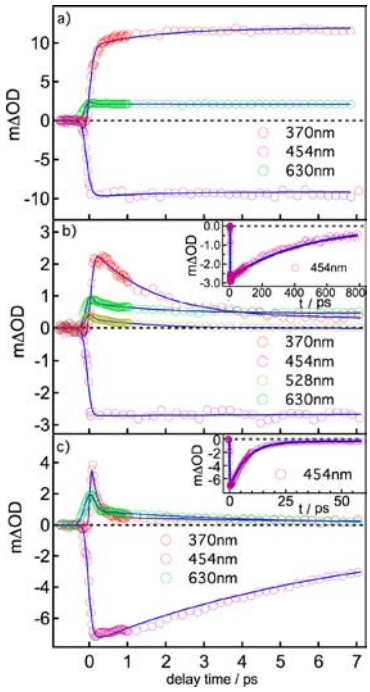

Figure 2. Time profiles at different wavelengths for (a) $[Ru(bpy)_3]^{2+}$, (b) $[Ru(m\text{-}bpy)_3]^{2+}$, and (c) $[Ru(tm\text{-}bpy)_3]^{2+}$. Insets: corresponding ground-state recovery at 454 nm. Symbols, experimental; lines, least-squares fits.

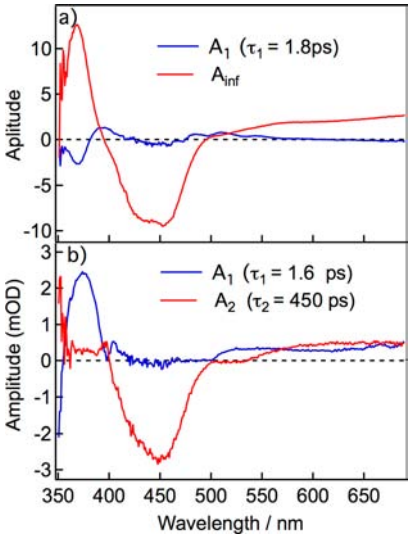

Figure 3. Decay-associated difference absorption spectra from global analysis of the transient spectra for (a) $[Ru(bpy)_3]^{2+}$, fit function $f(t) = A_1 \exp(-t/\tau_1) + A_{inf}$, and (b) $[Ru(m\text{-}bpy)_3]^{2+}$, fit function $f(t) = A_1 \exp(-t/\tau_1) + A_2 \exp(-t/\tau_2)$.

vibrational cooling on the same time scale results in slightly time-dependent band shapes. However, bi-exponential fits at the wavelengths of the transient maxima and minima were satisfactory. In particular, the decay of the 360 nm signal as well as the ground-state recovery at 454 nm are even faster than for $[Ru(m\text{-}bpy)_3]^{2+}$, with values of τ_1 = 0.16 ps (comparable to the instrument response function) and τ_2 = 7.5 ps, respectively.

The conclusion is that, for $[Ru(m\text{-}bpy)_3]^{2+}$ and $[Ru(tm\text{-}bpy)_3]^{2+}$, the depopulation of the ^{3}MLCT state to an intermediate non-luminescent state occurs within a few

dx.doi.org/10.1021/ja407225t | J. Am. Chem. Soc. 2013, 135, 13660−13663

picoseconds. From the latter the system returns to the ground state more slowly. Two possibilities for this state offer themselves: (a) partial ligand dissociation and re-chelation, or (b) the ^{3}dd state. The former is not very likely, as this would also result in ESA signals in the region of the ground-state bleach[20] and re-chelation would be expected to be slower for the tm-bpy ligand because of higher steric hindrance. The rationale for the ^{3}dd state as intermediate state is the following: for $[Ru(m\text{-}bpy)_3]^{2+}$, the methyl group in the 6 position forces a slightly longer Ru−N bond to the corresponding N atom. This results in a reduction of the effective ligand-field strength, like in the analogous Fe(II) complex, which, in contrast to low-spin $[Fe(bpy)_3]^{2+}$, is a well-known spin-crossover complex.[21] A similar stabilization is expected for the ^{3}dd state in $[Ru(m\text{-}bpy)_3]^{2+}$ since, even though the metal−ligand bond length difference between the ground state and the ^{3}dd state is smaller than that between the low-spin and the high-spin states in iron(II) complexes. The effect of a bond length change in ruthenium complexes is enhanced due to the overall stronger ligand-field strength for 4d metal ions.

For $[Ru(tm\text{-}bpy)_3]^{2+}$ with methyl groups in both the 6 and the 6′ positions, the reduction of the ligand-field strength and therefore the stabilization of the ^{3}dd state are even larger. With this in mind, the qualitative diagram for the potential energy surfaces shown in Figure 4 can be proposed. For $[Ru(bpy)_3]^{2+}$,

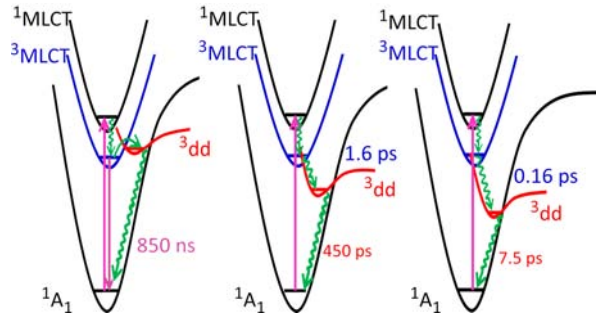

Figure 4. Schematic representation of the potential energy surfaces of the ground state and the relevant excited states of $[Ru(bpy)_3]^{2+}$, $[Ru(m\text{-}bpy)_3]^{2+}$, and $[Ru(tm\text{-}bpy)_3]^{2+}$ (from left to right). Radiative and non-radiative processes are indicated by smooth and wavy lines, respectively.

the ^{3}dd state is, as is well accepted in the literature,[2,9,22] higher in energy than the ^{3}MLCT state. For both of the other two complexes, the ^{3}dd state lies lower in energy than the ^{3}MLCT state, but more so for $[Ru(tm\text{-}bpy)_3]^{2+}$. In all cases, the ISC from the initially excited ^{1}MLCT to the ^{3}MLCT state is assumed to take ∼50 fs, as determined for $[Ru(bpy)_3]^{2+}$.[11,12] For this complex, thermally activated quenching of the ^{3}MLCT luminescence at higher temperatures is possible, during which the population of the ^{3}dd state remains negligible at all times. Therefore, the absorptions characteristic of the ^{3}MLCT state and the ground-state recovery occur with the same time constant.[19] For $[Ru(m\text{-}bpy)_3]^{2+}$ and $[Ru(tm\text{-}bpy)_3]^{2+}$, the ^{3}MLCT signature disappears with τ_1 = 1.6 and 0.16 ps, respectively. This is attributed to internal conversion from the ^{3}MLCT to the ^{3}dd state, which is now exergonic. The crossing points of the potential energy surfaces are such that it is in the strong vibronic coupling limit. Therefore, the internal conversion is faster for the more exergonic case, that is, for $[Ru(tm\text{-}bpy)_3]^{2+}$. In the latter case, 0.16 ps reflects a combination of the ^{1}MLCT to ^{3}MLCT ISC, charge localization, solvent reorganization, the onset of vibrational relaxation, and the internal conversion to the ^{3}dd state. The ISC process, by which the complex reverts back to ground state, is in the intermediate to weak coupling limit. It thus obeys the classic energy gap law, and therefore it is again faster for $[Ru(tm\text{-}bpy)_3]^{2+}$ than for $[Ru(m\text{-}bpy)_3]^{2+}$.

The DADS for $[Ru(m\text{-}bpy)_3]^{2+}$ (Figure 3b) reveal another interesting point. The amplitude A_1 of the fast component is very similar to that of the long component A_{inf} for $[Ru(bpy)_3]^{2+}$ in the region of the characteristic absorptions of the ^{3}MLCT state, that is, between 350 and 400 nm and above 500 nm. The amplitude A_2 of the slow component also shows absorption of the intermediate state in the form of a weak and broad band above 530 nm in addition to the ground-state bleaching. This is attributed to ESA from the $^3T_1(t_{2g}^5e_g^1)$ state. With an intensity roughly 1 order of magnitude smaller than that of the ^{1}MLCT transition, this band can be attributed to a spin-allowed MLCT transition of the ^{3}dd state. It is weaker and broader than the ^{1}MLCT transition because in the ^{3}dd state the Ru−N bond distances are significantly longer than in the ground state.

The above is supported by the experimental determination of the crystal structures, in particular the Ru−N bond lengths of the three complexes, and by results from density functional theory (DFT) calculations (see SI for computational details). As the X-ray structure of $[Ru(tm\text{-}bpy)_3]^{2+}$ could not be determined because of insufficient quality of the crystals, that of $[Ru(dm\text{-}bpy)_3]^{2+}$ (dm-bpy = 6,6′-dimethyl-2,2′-bipyridine) is reported instead. DFT calculations on both complexes indicate that the peripheral methyl groups in $[Ru(tm\text{-}bpy)_3]^{2+}$ have a minor influence and that therefore $[Ru(dm\text{-}bpy)_3]^{2+}$ is a good model for the former with respect to the relevant structural and energetic parameters. Experimental and calculated ground-state geometries show good agreement (see SI for details). Furthermore, the DFT results agree well with recently published high-level computational results on ruthenium(II) tris-diimine complexes.[23] Table 1 shows the average Ru−N

Table 1. Experimental[a] and DFT[b] Optimized Average Ru−N Bond Lengths (Å) of $[Ru(L)_3]^{2+}$ (L = bpy, m-bpy, dm-bpy, tm-bpy) in the S_0 and ^{3}dd States, and Calculated Excited-State/Ground-State Zero-Point Energy Differences $\Delta E°$ (cm^{-1})

		bpy	m-bpy	dm-bpy	tm-bpy
d(Ru−N)	S_0/exp	2.065[26a]	2.089[26b]	2.127[26b]	–
	S_0/calc	2.090	2.122	2.154	2.153
	^{3}dd/calc	2.227	2.235	2.306	2.307
	^{3}MLCT/calc	2.090	2.121	–	–
$\Delta E°$ [c]	^{3}MLCT	15007	14521	–	–
	^{3}dd	17932	14101	11218	11034

[a]For full structure reports see SI. [b]Computational geometries with CP2K; similar results are obtained with G09. [c]Gas-phase values; inclusion of solvent does not change these significantly (for details see SI).

bond lengths for experimental and calculated geometries, illustrating that the ground-state bond lengths are indeed slightly longer for the Ru−N bonds with an adjacent methyl group. Also, the bond-length difference between the ground state and the ^{3}MLCT state is very small, in agreement with experiment,[24] whereas that between these two and the ^{3}dd state is substantial. The ^{3}dd state, with its unpaired electron in the e_g orbitals, is Jahn−Teller active, as becomes evident from the

dx.doi.org/10.1021/ja407225t | J. Am. Chem. Soc. 2013, 135, 13660−13663

strongly distorted optimized structures in this state with one Ru−N distance of as much as ∼2.9 Å for $[Ru(dm\text{-}bpy)_3]^{2+}$ and $[Ru(tm\text{-}bpy)_3]^{2+}$ (see SI for details). Although DFT is sensitive with regard to absolute energy differences for states of different spin multiplicities, it provides very good relative energies for the same spin state in different compounds.[25] Thus, DFT predicts a stabilization of the ^{3}dd energy on going from $[Ru(bpy)_3]^{2+}$ to $[Ru(m\text{-}bpy)_3]^{2+}$ by ∼4000 cm^{-1} and by another ∼3000 cm^{-1} on going to both $[Ru(dm\text{-}bpy)_3]^{2+}$ and $[Ru(tm\text{-}bpy)_3]^{2+}$, putting it definitely below the ^{3}MLCT state for those two (Table 1).

The above is also consistent with photo-dissociation experiments performed on the three complexes for irradiation at 405 nm (for details see SI). The quantum efficiencies for ejection of a ligand are 2.4×10^{-4} for $[Ru(bpy)_3]^{2+}$, 2.7×10^{-3} for $[Ru(m\text{-}bpy)_3]^{2+}$, and 2.5×10^{-4} for $[Ru(tm\text{-}bpy)_3]^{2+}$. The value for the parent $[Ru(bpy)_3]^{2+}$ complex is consistent with data from the literature.[1] The quantum efficiency is related to the lifetime of the transient ^{3}dd state. It is 1 order of magnitude higher for $[Ru(m\text{-}bpy)_3]^{2+}$, with a lifetime of 450 ps for the ^{3}dd state, as compared to 7.5 ps for $[Ru(tm\text{-}bpy)_3]^{2+}$.

In conclusion, we have identified a comparatively long-lived intermediate state in the relaxation cascade of non-luminescent ruthenium(II) tris-bipyridyl complexes, and we attribute it to the lowest energy ^{3}dd state. This is quite an important finding, as to date it has been tacitly assumed that the lifetime of this state was much shorter than the internal conversion process feeding it. This is of even greater significance, for instance, in the optimization of the photo-decomposition in the proposed application of ruthenium(II)-based polypyridyl complexes in anticancer therapy.[7,8]

■ ASSOCIATED CONTENT

Ⓢ Supporting Information

Details of the structure determination, computational results, and photo-dissociation experiments. This material is available free of charge via the Internet at http://pubs.acs.org.

■ AUTHOR INFORMATION

Corresponding Author

andreas.hauser@unige.ch

Author Contributions

[§]Q.S. and S.M.-V. contributed equally.

Notes

The authors declare no competing financial interest.

■ ACKNOWLEDGMENTS

We thank the Swiss National Science Foundation (Grant Nos. 200020-137567 and the NCCR MUST) for financial support and the CSCS for computational resources.

■ REFERENCES

(1) Durham, B.; Caspar, J. V.; Nagle, J. K.; Meyer, T. J. *J. Am. Chem. Soc.* **1982**, *104*, 4803.

(2) Sauvage, J. P.; Collin, J. P.; Chambron, J. C.; Guillerez, S.; Coudret, C.; Balzani, V.; Barigelletti, F.; Decola, L.; Flamigni, L. *Chem. Rev.* **1994**, *94*, 993.

(3) Zayat, L.; Calero, C.; Albores, P.; Baraldo, L.; Etchenique, R. *J. Am. Chem. Soc.* **2003**, *125*, 882.

(4) Borg, O. A.; Godinho, S.; Lundqvist, M. J.; Lunell, S.; Persson, P. *J. Phys. Chem. A* **2008**, *112*, 4470.

(5) Salassa, L.; Garino, C.; Salassa, G.; Gobetto, R.; Nervi, C. *J. Am. Chem. Soc.* **2008**, *130*, 9590.

(6) Grätzel, M. *Inorg. Chem.* **2005**, *44*, 6841.

(7) Higgins, S. L. H.; Brewer, K. J. *Angew. Chem., Int. Ed.* **2012**, *51*, 11420.

(8) (a) Howerton, B. S.; Heidary, D. K.; Glazer, E. C. *J. Am. Chem. Soc.* **2012**, *134*, 8324. (b) Wachter, E.; Heidary, D. K.; Howerton, B. S.; Parkin, S.; Glazer, E. C. *Chem. Commun.* **2012**, *48*, 9649.

(9) Van Houten, J.; Watts, R. J. *J. Am. Chem. Soc.* **1976**, *98*, 4853.

(10) Osterman, T.; Abrahamsson, M.; Becker, H. C.; Hammarstrom, L.; Persson, P. *J. Phys. Chem. A* **2012**, *116*, 1041.

(11) Damrauer, N. H.; Cerullo, G.; Yeh, A.; Boussie, T. R.; Shank, C. V.; McCusker, J. K. *Science* **1997**, *275*, 54.

(12) (a) Cannizzo, A.; van Mourik, F.; Gawelda, W.; Zgrablic, G.; Bressler, C.; Chergui, M. *Angew. Chem., Int. Ed.* **2006**, *45*, 3174. (b) Bhasikuttan, A. C.; Suzuki, M.; Nakashima, S.; Okada, T. *J. Am. Chem. Soc.* **2002**, *124*, 8398. (c) Kukura, P.; McCamant, D. W.; Mathies, R. A. *Annu. Rev. Phys. Chem.* **2007**, *58*, 461.

(13) (a) Wallin, S.; Davidsson, J.; Modin, J.; Hammarstrom, L. *J. Phys. Chem. A* **2005**, *109*, 4697. (b) Yeh, A. T.; Shank, C. V.; McCusker, J. K. *Science* **2000**, *289*, 935.

(14) (a) Damrauer, N. H.; McCusker, J. K. *J. Phys. Chem. A* **1999**, *103*, 8440. (b) Henry, W.; Coates, C. G.; Brady, C.; Ronayne, K. L.; Matousek, P.; Towrie, M.; Botchway, S. W.; Parker, A. W.; Vos, J. G.; Browne, W. R.; McGarvey, J. J. *J. Phys. Chem. A* **2008**, *112*, 4537.

(15) Winkler, J. R.; Netzel, T. L.; Creutz, C.; Sutin, N. *J. Am. Chem. Soc.* **1987**, *109*, 2381.

(16) Hewitt, J. T.; Vallett, P. J.; Damrauer, N. H. *J. Phys. Chem. A* **2012**, *116*, 11536.

(17) Suzuki, K.; Kobayashi, A.; Kaneko, S.; Takehira, K.; Yoshihara, T.; Ishida, H.; Shiina, Y.; Oishi, S.; Tobita, S. *Phys. Chem. Chem. Phys.* **2009**, *11*, 9850.

(18) McCusker, J. K. *Acc. Chem. Res.* **2003**, *36*, 876.

(19) (a) Tarnovsky, A. N.; Gawelda, W.; Johnson, M.; Bressler, C.; Chergui, M. *J. Phys. Chem. B* **2006**, *110*, 26497. (b) Müller, P.; Brettel, K. *Photochem. Photobiol. Sci.* **2012**, *11*, 632. (c) Thompson, D. W.; Wishart, J. F.; Brunschwig, B. S.; Sutin, N. *J. Phys. Chem. A* **2001**, *105*, 8117.

(20) Liu, Y.; Turner, D. B.; Sing, T. N.; Angeles-Boza, A. M.; Chouai, A.; Dunbar, K. R.; Turro, C. *J. Am. Chem. Soc.* **2009**, *131*, 26.

(21) Goodwin, H. A.; Sylva, R. N. *Aust. J. Chem.* **1968**, *21*, 83.

(22) Islam, A.; Ikeda, N.; Yoshimura, A.; Ohno, T. *Inorg. Chem.* **1998**, *37*, 3093.

(23) Alary, F.; Heully, J. L.; Bijeire, L.; Vicendo, P. *Inorg. Chem.* **2007**, *46*, 3154.

(24) Gawelda, W.; Johnson, M.; de Groot, F. M.; Abela, R.; Bressler, C.; Chergui, M. *J. Am. Chem. Soc.* **2006**, *128*, 5001.

(25) Lawson Daku, L. M.; Aquilante, F.; Robinson, T. W.; Hauser, A. *J. Chem. Theory Comput.* **2012**, *8*, 4216.

(26) (a) Rillema, D. P.; Jones, D. S.; Woods, C.; Levy, H. A. *Inorg. Chem.* **1992**, *31*, 2935. (b) Onggo, D.; Scudder, M. L.; Craig, D. C.; Goodwin, H. A. *J. Mol. Struct.* **2005**, *738*, 129.